

Spotless days and geomagnetic index as the predictors of solar cycle 25

Dipali S. Burud^{1,9}, Rajmal Jain², Arun K. Awasthi^{3,4}, Sneha Chaudhari⁹, Sushanta C. Tripathy⁵, Nat Gopalswamy⁶, Pramod Chamadia⁷, Subhash C. Kaushik⁸ and Rajiv Vhatkar¹

¹ Department of Physics, Shivaji University, Kolhapur 416004, India

² Physical Research Laboratory, Navrangpura, 380009 Ahmedabad; profrajmaljain9@gmail.com

³ CAS Key Laboratory of Geospace Environment, Department of Geophysics and Planetary Sciences, University of Science and Technology of China, Hefei 230026, China

⁴ CAS Key Laboratory of Solar Activity, National Astronomical Observatories, Beijing 100101, China

⁵ National Solar Observatory, 3665 Discovery Drive, Boulder, CO 80303, USA

⁶ Goddard Space Flight Center, NASA, Greenbelt, MD 20771, USA

⁷ Department of Physics, Govt. P. G. College, Satna, M. P., 485001, India

⁸ Department of Physics, Govt. PG Autonomous College, Datiya, M. P., 475661, India

⁹ Sh. M. M. Patel Institute of Sciences and Research, Kadi Sarva Vishwavidyalaya, Gandhinagar 382015, India

Received 2020 November 11; accepted 2021 April 9

Abstract We study the sunspot activity in relation to spotless days (SLDs) during the descending phase of solar cycles 11–24 to predict the amplitude of sunspot cycle 25. For this purpose, in addition to SLD, we also consider the geomagnetic activity (*aa* index) during the descending phase of a given cycle. A very strong correlation of the SLD (0.68) and *aa* index (0.86) during the descending phase of a given cycle with the maximum amplitude of next solar cycle has been estimated. The empirical relationship led us to deduce the amplitude of cycle 25 to be 99.13 ± 14.97 and 104.23 ± 17.35 using SLD and *aa* index, respectively as predictors. Both the predictors provide comparable amplitude for solar cycle 25 and reveal that solar cycle 25 will be weaker than cycle 24. Further, we predict that the maximum of cycle 25 is likely to occur between February and March 2024. While the *aa* index has been utilized extensively in the past, this work establishes SLDs as another potential candidate for predicting the characteristics of the next cycle.

Key words: Sun: activity — Sun: sunspots — Sun: rotation — methods: statistical

1 INTRODUCTION

The magnetic field is generated in the solar interior through the dynamo mechanism via the motion of plasma and is seen as dark spots with strong magnetic fields. These observed sunspots are varying in number between 0 (lowest) and 250 (highest) with approximately an 11 year period, well known as the Schwabe cycle. The solar cycles are characterized by their length, amplitude, rise time, fall time, etc. The solar activities such as sunspot number, sunspot areas, total solar irradiance, coronal mass ejection (CME), solar flares, facular area and 10.7 cm solar radio flux ($F_{10.7}$) exhibit cyclic behavior as observed by various researchers (Jain 1986, 1997; Krivova & Solanki 2002; Braun et al. 2005; Ataç et al. 2006; Kilcik et al. 2010, 2012; Hathaway et al. 2002; Javaraiah 2019; El-Borie et al. 2020). The period of the Schwabe cycle varies between 7.4

and 14.8 yr, with the ascending and descending phase of 4–5 and 5–6 yr, respectively (Usoskin & Mursula 2003). These types of periodicity are very useful in understanding solar phenomena which can affect long-term changes in climate and short-term changes in space weather (Nandy & Martens 2007).

In a given solar cycle, there are many days without sunspots, which are known as spotless days (SLDs). The number of SLDs in a year or in a given cycle can be obtained from the website (www.sidc.be/silso/datafiles) which covers the period 1818 January 1 to December 2020. The SLDs are generally noted during the descending phase and reach maximum in a sunspot minimum year. SLDs are also found to be present during a maximum year. The highest number of SLDs (311) occurred in the year 1913 of cycle 14. The maximum number of SLDs (973) in a given cycle was found in cycle

Table 1 Occurrence Frequency of SLD for the Descending Phase of Solar Cycle 11–24

Consecutive Days	Occurrence frequency	Consecutive Days	Occurrence frequency	Consecutive Days	Occurrence frequency
1	264	16	9	31	4
2	140	17	7	36	2
3	113	18	7	37	2
4	86	19	9	39	1
5	60	20	7	40	2
6	50	21	6	42	1
7	40	22	4	43	1
8	38	23	2	44	1
9	31	24	5	45	1
10	25	25	3	47	1
11	17	26	6	49	1
12	17	27	6	69	1
13	22	28	1	92	1
14	15	29	1		
15	20	30	3		

12. The total numbers of SLD in cycle 23 (August 1996 to 2019 December 31) are found to be 573, similar to cycle 15 (556) and cycle 16 (541). However cycle 24 showed a total of 913 SLDs until December 2019 (Burud et al. 2021, in preparation).

The highest value of SLD in a given cycle has been used to define the minimum phase of the corresponding cycle by Waldmeier (1961) and McKinnon & Waldmeier (1987). These authors suggested that the date of sunspot minimum can be decided by the number of SLDs. Wilson (1995) utilized the timing of occurrence of the first observed SLD in a given cycle with various other timings such as time period between the solar minimum to the first SLD observation after the solar maximum, time period between the solar maximum to the first SLD observation after the solar maximum, etc., to predict the minimum period of solar cycle 22. A similar result has been observed by Hamid & Galal (2006) and Carrasco et al. (2016). Harvey & White (1999) demonstrated that the SLD is not the only parameter to decide the minimum of a solar cycle but other parameters such as the monthly averaged sunspot number, the number of regions (total, new- and old-cycle), etc., need to be considered. Helal & Galal (2013a) indicated that the relation between the SLDs along two year intervals around the preceding minimum can be used to predict the amplitude of the next solar cycle and obtained a value of 118.2 for cycle 25.

Further, the geomagnetic activity (*aa* index) during the descending phase of a given sunspot cycle provides an asymptomatic prediction of the magnitude of annual mean sunspot number in the next sunspot cycle (Jain 1997). Employing the *aa* index as a predictor, Jain (1997) estimated the amplitude of solar cycle 23 to be 166.2, which is found to be in agreement with the observed value of 173.4. However, it may be noted that Jain (1997) extended the period of descending phase to five years (minimum plus previous four years) to predict the

amplitude and timing of the next solar cycle as predictor. Further, it would be interesting to explore the relationship between the two predictors: SLD and *aa* index.

In this paper, we carry out a statistical analysis of SLD and *aa* index during the descending phases of solar cycles 11 to 24, to investigate the characteristics of solar cycle 25. This paper is organized as follows: in Section 2 we give sources, description of the data, analysis and results are presented in Section 3 and discussions and brief conclusions are presented in Sections 4 and 5 respectively.

2 SOURCES OF DATA

We consider the sunspot number (R) that has recently been published and obtained from the SILSO website to study the physical properties of SLD from solar cycles 6 to 24 (Wilson et al. 1996; Li et al. 2005). The SLD data are taken for the period January 1868 to December 2019 covering cycles 11 to 24 since the *aa* index is available for the period. In order to minimize the inconsistency in calendar years related to sunspots numbers (see Petrovay 2020), a 13-month boxcar average of monthly mean sunspot numbers is calculated as follows

$$R_m = \frac{1}{24}(R_{i,-6} + 2 \sum_{j=-5}^{j=5} R_{i,j} + R_{i,6}) \quad (1)$$

where R_m is the 13-month smoothed maximum annual mean sunspot number which is calculated by using the mean of monthly sunspot numbers (R_j) over 13 months centered on the corresponding month (R_i).

The *aa* index has been taken from a British geological survey where the data are available from 1868 at www.geomag.bgs.ac.uk/data_service/data/magnetic_indices/aaindex. The *aa* index provides a daily average level of geomagnetic activity measured in nT. Eight datasets of 3-hourly values of *aa* index are averaged to obtain the daily *aa* index for a

Table 2 Yearwise comparison of R_m , no. of SLD and sum of aa index ($\sum aa$) over descending phases of solar cycles 21, 22, 23 and 24.

cycle 21			cycle 22			cycle 23			cycle 24						
Year	R_m	SLD	$\sum aa$	Year	R_m	SLD	$\sum aa$	Year	R_m	SLD	$\sum aa$	Year	R_m	SLD	$\sum aa$
1982	114.28	0	98782	1992	93.85	0	79691	2004	41.90	3	67475	2015	72.63	0	64945
1983	74.68	4	86134	1993	55.56	0	74251	2005	28.93	13	67653	2016	41.51	27	58315
1984	42.20	13	84635	1994	30.23	19	85515	2006	16.06	65	47211	2017	21.33	96	56635
1985	17.88	83	65833	1995	17.27	61	63906	2007	7.98	163	43628	2018	8.68	208	40438
1986	13.77	129	61308	1996	9.10	165	54244	2008	2.86	265	41277	2019	3.52	273	36404

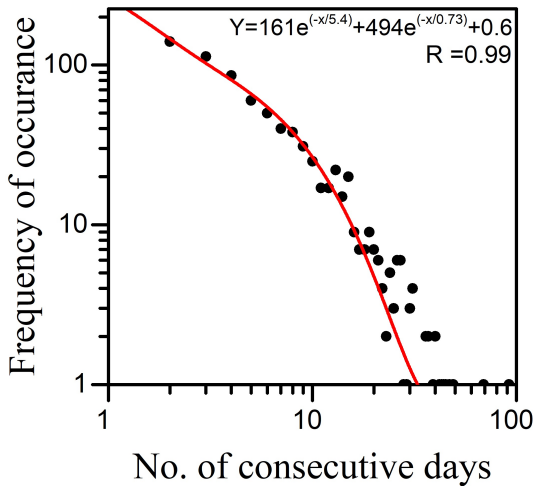


Fig. 1 Occurrence frequency of SLD as a function of number of consecutive SLDs during the descending phase of solar cycles 11 to 24.

given day. As mentioned earlier, the aa index is taken for the period January 1868 to December 2019, representing cycles 11 to 24.

3 ANALYSIS AND RESULTS

3.1 Prediction of the 13-month Smoothed Maximum Annual Mean Sunspot Number

The SLD data are taken from a website maintained by the Solar Influences Data Center (SIDC), at the Royal Observatory of Belgium. It is also observed that the SLD can occur between two days when the sunspots have been located on the solar disk. Generally, during the descending phase of the solar cycle, we have observed that there are many continuous days without sunspots. We define such a continuous period of days observed as consecutive SLDs. Our data on SLD show that consecutive days are between 1 to 92 d, as presented in Table 1. This table allows us to study the occurrence frequency of the SLD distribution with respect to the number of consecutive days. As displayed in Figure 1, we find the distribution follows a negative exponential function.

Table 2 represents the yearwise comparison of parameters such as 13 month smoothed annual mean

sunspot number (R_m), number of SLDs and sum of aa index ($\sum aa$) over the descending phases of cycles 21, 22, 23 and 24.

Table 2 reveals that the total number of SLDs ($\sum SLD$) of the descending phase of cycle 22 is 1.06 times higher relative to cycle 21, and, similarly, cycle 23 is 2.07 times larger relative to cycle 22. This trend of increment in the value of SLD has also been observed in the current cycle 24, in which the SLD of its descending phase is 1.18 times higher relative to cycle 23. This indicates the upward trend in the number of SLDs, while 13-month smoothed monthly sunspot number (R_m) and sum of aa index ($\sum aa$) exhibits a downward trend for the long term cycle that began from cycle 21. This suggests that the Sun is heading towards a modern minimum in the Gleissberg cycle (Feynman & Gabriel 1990).

Further in this study, following the technique proposed in Jain (1997), Wang & Sheeley (2009), and Bhatt et al. (2009) we define the descending phase of a given n^{th} cycle to be spanning a period of five years, which comprises the minimum year and preceding four years. Subsequently, representative aa index and SLD values of the n^{th} cycle have been estimated by integrating over the entire descending phase duration of five years due to the following reason. Based on the examination of the polarity of the active regions and identification of the location of the ephemeral regions, Harvey (1992) proposed that the overlap between the two cycles is five years. Further, based on a statistical investigation of the time-series observations of 128 years, Jain (1997) found that the aa index averaged over the period of five years is the effective precursor for estimating the characteristics of the next solar cycle. A total number of aa index ($\sum aa_{dsc}$) and SLDs ($\sum SLD_{dsc}$), integrated over the descending phase of the n^{th} cycle for cycles 11 to 24, is given in Table 3.

Shown in Figure 2 is the 13 month smoothed maximum annual mean sunspots number (R_{max}) of the $(n + 1)^{\text{th}}$ cycle plotted as a function of observed number of total SLDs during the descending phase ($\sum SLD_{dsc}$) of the n^{th} cycle. The best χ^2 linear fit to the data indicates a correlation coefficient of 0.68, which leads us to derive an empirical relation between these two indices for cycles

Table 3 Parameters of Solar Cycles 11–24

Cycle no.	Descending years	$(\sum SLD)_{dsc}$	$\sum SLD$	$(\sum aa)_{dsc}$	R_{max}		
					Observed	Calculated by SLD (error in %)	Calculated by aa (error in%)
11	1874–1878	753	806	151672	140	-	-
12	1886–1890	699	973	221763	72.5	85.42(17.8)	67.8(6)
13	1898–1902	845	909	141825	87.9	90.39(2.8)	91.7(4)
14	1909–1913	846	903	199465	64.2	76.96(20)	64.5(0.5)
15	1919–1923	387	556	250574	105.4	76.86(27)	84.1(20)
16	1929–1933	394	541	293386	78.1	119.09(52)	101.5(30)
17	1940–1944	253	427	333868	119.2	118.45(0.6)	116.06(2.6)
18	1950–1954	398	414	352692	151.7	131.42(13.4)	129.8(14)
19	1960–1964	149	197	337074	201.3	118.08(41)	136.22(32)
20	1972–1976	247	325	362000	110.6	140.9(27)	130.9(18)
21	1982–1986	229	254	396692	164.5	131.97(19.7)	139.3(15)
22	1992–1996	245	289	357607	158.5	133.63(15.6)	151.2(4.6)
23	2004–2008	509	573	267244	120.8	132.16(9.4)	137.8(14)
24	2015–2019	604	913	256737	110.44	107.87(2.3)	107.17(2.9)
25						99.13 14.97	104.23 17.35

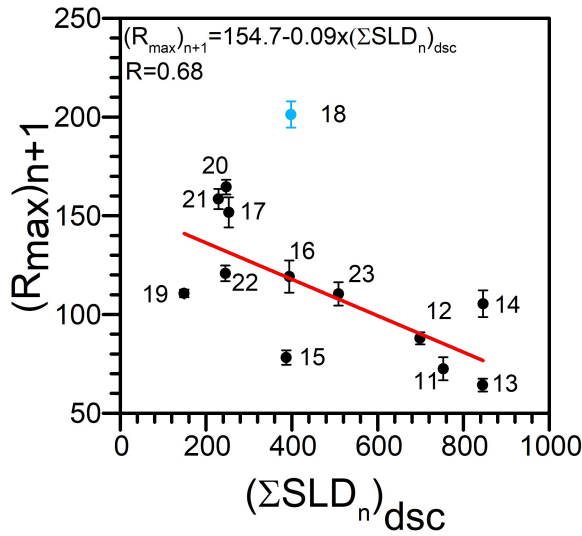


Fig. 2 The 13 month smoothed maximum annual mean sunspot number (R_{max}) of the $(n + 1)^{th}$ cycle plotted as a function of $(\sum SLD)_{dsc}$ for the n^{th} cycle. The data point corresponding to sum of the SLDs in the descending phase of cycle 18 ($\sum SLD)_{18}$ and maximum amplitude of sunspot number (R_{max}) of cycle 19, marked with point #18, has been excluded from the fitting equation.

11–24 as follows.

$$(R_{max})_{n+1} = 154.70 - 0.092(\sum SLD_n)_{dsc} \pm 14.97 \quad (2)$$

where $(R_{max})_{n+1}$ is the predicted 13 month smoothed maximum annual mean sunspot number of the $(n + 1)^{th}$ cycle.

From Figure 2, it is evident that point #18 (corresponding to R_{max} of cycle 19 and SLDs in the descending phase of cycle 18) is an obvious outlier and thus has been excluded in obtaining the empirical relation (1). A similar behavior of point #18 is also noted in Figure 3, in which the correlation of R_{max} of the preceding cycle is obtained against integrated aa index. This may be

attributed to either an underestimation of SLD and aa index, or an unusually high magnetic field activity in cycle 19 ($R_{max}=201$) compared to all of the investigated cycles where the maximum value of R_{max} has reached only a level of 164.5. The reason for this anomalous activity exhibited by predictors of cycle 18 has been investigated in detail by Wang & Sheeley (2009). They attributed an underestimation of the aa index (and radial interplanetary magnetic field (IMF) strength which is derived from the aa index) to cause this unusual behavior. Based on higher polar field strengths as estimated by Sheeley (2008), and a low-level of sunspot activity in 1954 (the end of cycle 18), they further argued that radial IMF strength and, thus, aa index have been underestimated. This led to the exclusion of point #18 from the correlation trend. In another investigation by Podladchikova et al. (2017), who established a correlation between the maximum amplitude of the solar cycle and temporal behaviors of the sunspot number during the declining phase of the preceding cycle in the form of “integral activity” which is the area under the sunspot cycle curve. After studying solar cycles 10–23, they found a slow declining trend in the sunspot number, which exhibited a sudden increase during the years 1950–1954 (i.e., descending phase of cycle 18). Since the rate of decline of sunspots has decreased in this duration, they attributed this to cause a higher value of R_{max} for cycle 19. This unusual behavior of cycle 19 led to its exclusion from further investigations by other investigators, Petrovay (2010) and Clilverd et al. (2006).

The total number of observed SLDs in the descending phase of cycle 24 is $(\sum SLD_{24})_{dsc} = 604$, which yields $(R_{max})_{25} = 99.13 \pm 14.97$ using Equation (2). This indicates that the amplitude of cycle 25 will be lower than that of cycle 24, $(R_{max})_{24} = 110.44$.

Further, aa index during the descending phase of a given cycle has been found to be a good predictor of the

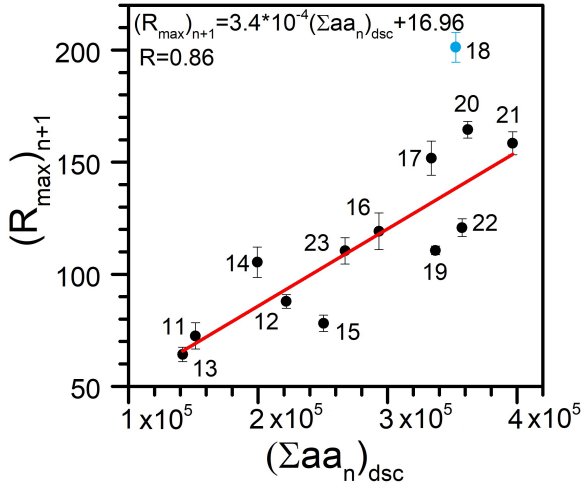


Fig. 3 The 13 month smoothed maximum annual mean sunspot numbers (R_{max}) of the $(n + 1)^{\text{th}}$ cycle plotted as a function of $(\sum aa)_{dsc}$ of the n^{th} cycle. The correlation between them is 0.86. The data point corresponding to the sum of the aa index in the descending phase of cycle 18 $(\sum aa)_{18}$ and maximum amplitude of sunspot number (R_{max}) of cycle 19, marked with point #18, has been excluded from the fitting equation.

amplitude of the following cycle (Ohl 1966; Jain 1997; Lantos & Richard 1998; Hathaway et al. 1999; Hathaway 2009; Wang & Sheeley 2009; Bhatt et al. 2009). In order to apply the prediction scheme similar to that employed in the previous section on SLDs, we calculate the total value of aa index $(\sum aa)_{dsc}$ over the descending phase of the given n^{th} cycle. We provide the result in Table 3 for solar cycles 11 to 24.

In Figure 3, we display the relation between 13 month smoothed maximum annual mean sunspot numbers (R_{max}) of $(n + 1)^{\text{th}}$ cycle and $(\sum aa)_{dsc}$ of the n^{th} cycle. The linear fit with a correlation coefficient (0.86) is found with the following empirical relation.

$$(R_{max})^{n+1} = 3.4 \times 10^{-4} (\sum aa_n)_{dsc} + 16.96 \pm 17.35 \quad (3)$$

where $(R_{max})_{n+1}$ is the predicted 13 month smoothed maximum annual mean sunspot number for the $(n + 1)^{\text{th}}$ cycle.

Considering cycle 24 to have ended in December 2019, according to www.sidc.be/silso/datafiles/node/166, we obtain $(\sum aa_{dsc}) = 256737$. Using this value in relation (2), we obtain $(R_{max})_{25} = 104.23 \pm 17.35$. This value of R_{max} , derived from the aa index as the predictor, agrees well with that derived using SLD as a predictor (99.13 ± 14.97). Therefore, this work identifies the potential of SLD as the precursor of the next solar cycle. Further, we are able to confirm that cycle 25 will be weaker than cycle 24.

Table 3 gives a comparison between the observed and calculated values of the 13 month smoothed maximum annual mean sunspot numbers for both the precursor methods. The comparative analysis indicates that in some cases, the calculated values from relation (2) agree well (relative to those calculated from relation (3)) with the observed values of R_{max} (for cycles 23 and 24) whereas vice-versa for others. Therefore, we find that, in general, the calculated values of R_{max} from both the relations agree well with the observed values.

3.2 Prediction of the Maximum Period of Solar Cycle 25

According to the Waldmeier effect (Waldmeier 1935) and our findings that solar cycle 25 will be weaker, it is clear that the ascending phase of cycle 25 is expected to be longer in duration. Thus it is important to predict the ascending period of cycle 25. For this purpose, we explore the relationship between the ascending phase and period in years, $(P_{asc})_n$ and $(R_{max})_n$. Presented in Figure 4 is the plot between $(P_{asc})_n$ and $(R_{max})_n$ for cycles 11–24. The best fit line corresponds to a correlation value of -0.78 . The trend reveals that $(P_{asc})_n$ of a solar cycle decreases with the increase in $(R_{max})_n$, representing manifestation of the “Waldmeier effect”. The linear fit is expressed in the form of the following empirical relation

$$(P_{asc})_n = 5.7 - 0.015(R_{max})_n \pm 0.43. \quad (4)$$

On substituting the value of $(R_{max})_{25} = 99.13 \pm 14.97$, derived from the SLD technique, we obtain $(P_{asc})_{25} = 4.21 \pm 0.43$ yr. On the other hand, by substituting $(R_{max})_{25} = 104.23 \pm 17.35$, obtained from the aa method, we estimate $(P_{asc})_n = 4.14 \pm 0.43$ yr. Results from both techniques reveal that ascending period for cycle 25 is likely to be around 4.17 ± 0.43 yr (the average of both techniques), which suggests the peak amplitude of cycle 25 is likely to occur between February and March 2024.

4 DISCUSSION

In the current investigation, we use SLDs during the descending phase of a given cycle to predict the sunspot amplitude of the next cycle. Based on this technique, we obtained maximum amplitude (R_{max}) for cycle 25 to be 99.13 ± 14.97 . In addition to SLD as a predictor of the sunspot cycle characteristics, we also regarded sum of aa index as another solar activity proxy and found amplitude to be 104.23 ± 17.35 . This is in good agreement with the amplitude estimated with SLD. Our predicted amplitude of sunspot number 99.13 ± 14.97 for cycle 25 is in agreement with the recent predictions made by a few other investigators (within the range of 82–140) (Upton

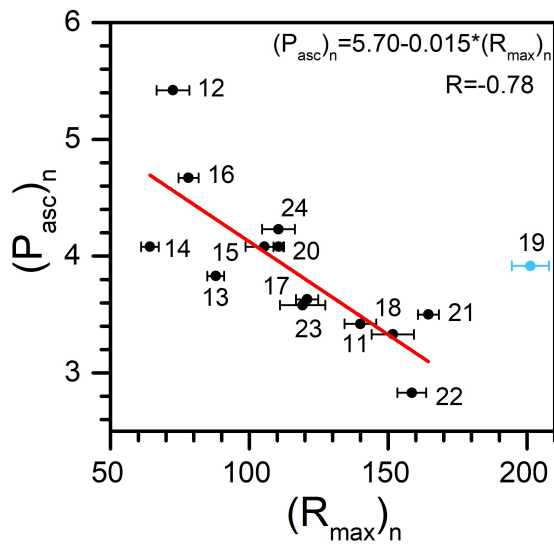


Fig. 4 The plot depicts the ascending phase of the n^{th} cycle as a function of 13 month smoothed maximum annual mean sunspot numbers (R_{max}) of the same cycle. The data point representing cycle 19 (marked by #19) has been excluded from the fitting equation.

& Hathaway 2018; Jiang et al. 2018; Bhowmik & Nandy 2018; Petrovay et al. 2018; Bisoi et al. 2020; Sello 2019; Dani & Sulistiani 2019; Covas et al. 2019; Labonville et al. 2019; Miao et al. 2020). On the other hand, some studies (Sarp et al. 2018; Li et al. 2018) contrarily predict cycle 25 to have a higher value (150–170). This difference may be attributed to different predictors as well as numerical schemes used (such as non-linear prediction algorithm (154) and bimodal distribution (168)). Thus, we find the amplitude of solar cycle 25 to be weaker than the current cycle 24. Further, the period of the peak amplitude of cycle 25 is predicted to be occurring between February and March 2024.

We have also shown in Table 2 that numbers of SLDs are continuously increasing while sum of aa index and sunspot numbers are decreasing from cycle 21. A total of 509 SLDs were observed during the descending phase of solar cycle 23, significantly higher than the values of 229 and 245 for solar cycles 21 and 22 respectively. On the other hand, in solar cycle 24, an extremely low sunspot activity during ascending (2009–2012) as well as descending phases (2015–2019) has been reported, and 604 SLDs have been observed. The continuous increases in numbers of SLD and sum of the aa index from cycle 21 and inferences from the current investigation reveal that cycles 24 and 25 are likely to be the part of the series of 2–4 successive weak and long cycles. This may suggest that the Sun has been progressing towards or is in the Gleissberg minimum or Grand Solar Minimum (Petrovay et al. 2018; Yousef 2003; Feynman & Gabriel 1990).

Considering the low amplitude of cycle 25 and decreasing trend of solar surface magnetic field, it is likely that cycle 26 may also be a weak cycle and if this trend continues, then it appears that the Sun may be heading towards the next Grand Solar Minimum. However, while our sunspot number predictions are in agreement with those obtained by several investigators in the past (see Table 4), they do not necessarily concur on our inference that the Sun appears to be heading towards a Grand Solar Minimum. For example, Bhowmik & Nandy (2018) predicted the maximum amplitude of the 25th cycle to be 118 with a peak in 2024, which is in agreement with our prediction. However, their ensemble forecast model indicates the reversal of weakening trend of solar activity.

It may be noted that the last Maunder Minimum was during 1645–1715 AD, and the end of upcoming cycle 26 would be nearly in 2043 AD, almost 400 years after the Maunder Minimum. Our above conclusions are further strengthened from the investigation carried out by Cameron et al. (2016) who showed that the measurements of the dipole moment of about 2 G at the end of cycle 23 are close to the simulated value of about 2.5 ± 1.1 G for cycle 25 in 2020. Based on the best correlation between the dipole moment during the solar minimum and the strength of the next solar cycle, Cameron et al. (2016) further suggested that cycle 25 will be of moderate amplitude, not much higher than that of the current cycle. It is widely known from several evidences that the strength of the Sun's polar fields near the time of a sunspot cycle minimum determines the strength of the following solar activity cycle. Hathaway & Upton (2016) applied their Advective Flux Transport code, with flows well constrained by observations, to simulate the evolution of the Sun's polar magnetic fields from early 2016 to the end of 2020, near the expected time of the cycle 24/25 minimum. Considering various limitations and uncertainties in simulations, they find that the average strength of the polar fields near the end of cycle 24 will be similar to that measured near the end of cycle 23, indicating that cycle 25 will be similar in strength to the current cycle 24. Further, Macario-Rojas et al. (2018) also showed that cycle 25 will be a weak solar cycle with slow rise time (14.4 per cent) and maximum activity (± 19.5 per cent) with respect to the current cycle 24. Table 4 summarizes the various predictions of several investigators for the amplitude of cycle 25. The table contains the author as well as year of publication, prediction method and predicted value in columns 1, 2 and 3 respectively. From the table, it is clear that our results concur with most of the previous investigators in the sense that solar cycle 25 has amplitude lower than the amplitude of solar cycle 24. On the other hand, there are few authors who claim

Table 4 Prediction for Cycle 25

Reference	Method	Maximum amplitude
Javaraiah (2017)	Cosine function + linear fit	30–40
Javaraiah (2015)	Maximum entropy method (MEM) and Morlet wavelet analysis.	50 ± 10
Covas et al. (2019)	Neural networks Spatiotemporal	57 ± 17
Kakad et al. (2017)	Shannon entropy model	63 ± 11.3
Labonville et al. (2019)	Solar dynamo models	89(+/- 29/14)
Attia et al. (2013)	Neural networks Neuro-fuzzy	90.7 ± 8
Gopalswamy et al. (2018)	Microwave imaging observations	89 and 59
Singh & Bhargawa (2019)	Extrapolation method	89 ± 9 and 78 ± 7
Kitiashvili et al. (2016)	Data assimilation method	90 ± 15
Jiang & Cao (2018)	SFT model	93 to 125
Chowdhury et al. (2021 accepted)	Precursor method Ap index	100.21 ± 15.06
Singh & Bhargawa (2017)	Hurst exponent	103 ± 25
Hiremath (2006)	Forced and damped harmonic oscillator model	110(±11)
Pishkalo (2019)	Polar field as precursor	116 ± 12
Hawkes & Berger (2018)	Magnetic helicity	117
Helal & Galal (2013b)	Precursor technique of spotless	118.2
Pesnell & Schatten (2018)	Employing solar dynamo index	135 ± 25
Du (2020)	Logarithmic relationship between R_m and aa	151.1 ± 16.9
Sarp et al. (2018)	Non-linear prediction algorithm	154 ± 12

that cycle 25 may be of similar or higher amplitude than cycle 24. Moreover, our results from both techniques (SLD and aa) fall within the uncertainty of the NOAA/NASA consensus predictions published on 2019 December 9 that strength of upcoming solar cycle 25 would be comparable to that of cycle 24 (<https://www.swpc.noaa.gov/news/solar-cycle-25-forecast-update>).

5 CONCLUSIONS

We have applied the available data for the SLD from cycles 11 to 24 (1874–2019). The occurrence frequency of SLD features a negative exponential distribution with respect to the consecutive days. A new prediction technique is proposed based on the number of SLDs observed in the declining phase of the solar cycle which demonstrates that the maximum of the 13 month smoothed maximum annual mean sunspot number for cycle 25 will be 99.13 ± 14.97 . The SLD occurrence density per cycle is found to increase from cycle 21 while sum of aa index and 13-month smoothed monthly sunspot number are decreasing during the descending phase of a cycle (cf. Table 2). This trend is indicative of weakening in the solar surface magnetic field of the Sun. In view of our analysis which resulted in the fact that solar cycle 25 is likely to be weaker in strength relative to the current cycle 24, we conclude that the Sun may be proceeding towards its next Grand Solar Minimum.

Acknowledgements Authors received the data for Sunspot Index and Long-term Solar Observations (SILSO) from the site of SIDC, WDC, Royal Observatory of Belgium. Cooperation received from President, KSV is sincerely acknowledged. RJ was invited by GSFC/NASA to work on this investigation. AKA acknowledges the

funding support from NSFC-11950410498 and KLSA-202010 grants. We earnestly thank the referee for valuable remarks which improved the paper.

References

- Ataç, T., Özgüç, A., & Rybak, J. 2006, *Sol. Phys.*, 237, 433
- Attia, A.-F., Ismail, H. A., & Basurah, H. M. 2013, *Ap&SS*, 344, 5
- Bhatt, N. J., Jain, R., & Aggarwal, M. 2009, *Sol. Phys.*, 260, 225
- Bhowmik, P., & Nandy, D. 2018, *Nature Communications*, 9, 5209
- Bisoi, S. K., Janardhan, P., & Ananthkrishnan, S. 2020, *Journal of Geophysical Research (Space Physics)*, 125, e27508
- Braun, H., Christl, M., Rahmstorf, S., et al. 2005, *Nature*, 438, 208
- Cameron, R. H., Jiang, J., & Schüssler, M. 2016, *ApJL*, 823, L22
- Carrasco, V. M. S., Aparicio, A. J. P., Vaquero, J. M., & Gallego, M. C. 2016, *Sol. Phys.*, 291, 3045
- Cilverd, M. A., Clarke, E., Ulich, T., et al. 2006, *Space Weather*, 4, S09005
- Covas, E., Peixinho, N., & Fernandes, J. 2019, *Sol. Phys.*, 294, 24
- Dani, T., & Sulistiani, S. 2019, in *Journal of Physics Conference Series*, 1231, 012022
- Du, Z. L. 2020, *Ap&SS*, 365, 104
- El-Borie, M. A., El-Taher, A. M., Thabet, A. A., et al. 2020, *ApJ*, 898, 73
- Feynman, J., & Gabriel, S. B. 1990, *Sol. Phys.*, 127, 393
- Gopalswamy, N., Mäkelä, P., Yashiro, S., & Akiyama, S. 2018, *Journal of Atmospheric and Solar-Terrestrial Physics*, 176, 26
- Hamid, R. H., & Galal, A. A. 2006, in *Solar Activity and its Magnetic Origin*, eds. V. Bothmer, & A. A. Hady, 233, 413
- Harvey, K. L. 1992, in *Astronomical Society of the Pacific Conference Series*, 27, *The Solar Cycle*, ed. K. L. Harvey, 335

- Harvey, K. L., & White, O. R. 1999, *J. Geophys. Res.*, 104, 19759
- Hathaway, D. H. 2009, *Solar Cycle Forecasting*, 32, *The Origin and Dynamics of Solar Magnetism*, 32 (Springer New York), 401
- Hathaway, D. H., & Upton, L. A. 2016, *Journal of Geophysical Research (Space Physics)*, 121, 10,744
- Hathaway, D. H., Wilson, R. M., & Reichmann, E. J. 1999, *J. Geophys. Res.*, 104, 22375
- Hathaway, D. H., Wilson, R. M., & Reichmann, E. J. 2002, *Sol. Phys.*, 211, 357
- Hawkes, G., & Berger, M. A. 2018, *Sol. Phys.*, 293, 109
- Helal, H. R., & Galal, A. A. 2013a, *Journal of Advanced Research*, 4, 275
- Helal, H. R., & Galal, A. A. 2013b, *Journal of Advanced Research*, 4, 275
- Hiremath, K. M. 2006, *A&A*, 452, 591
- Jain, R. 1986, *MNRAS*, 223, 877
- Jain, R. 1997, *Sol. Phys.*, 176, 431
- Javaraiah, J. 2015, *New Astron.*, 34, 54
- Javaraiah, J. 2017, *Sol. Phys.*, 292, 172
- Javaraiah, J. 2019, *Sol. Phys.*, 294, 64
- Jiang, J., & Cao, J. 2018, *Journal of Atmospheric and Solar-Terrestrial Physics*, 176, 34
- Jiang, J., Wang, J.-X., Jiao, Q.-R., & Cao, J.-B. 2018, *ApJ*, 863, 159
- Kakad, B., Kakad, A., & Ramesh, D. S. 2017, *Sol. Phys.*, 292, 181
- Kilcik, A., Özgüç, A., Rozelot, J. P., & Ataç, T. 2010, *Sol. Phys.*, 264, 255
- Kilcik, A., Yurchyshyn, V. B., Rempel, M., et al. 2012, *ApJ*, 745, 163
- Kitiashvili, I. N. 2016, *ApJ*, 831, 15
- Krivova, N. A., & Solanki, S. K. 2002, *A&A*, 394, 701
- Labonville, F., Charbonneau, P., & Lemerle, A. 2019, *Sol. Phys.*, 294, 82
- Lantos, P., & Richard, O. 1998, *Sol. Phys.*, 182, 231
- Li, F. Y., Kong, D. F., Xie, J. L., Xiang, N. B., & Xu, J. C. 2018, *Journal of Atmospheric and Solar-Terrestrial Physics*, 181, 110
- Li, K.-J., Gao, P.-X., & Su, T.-W. 2005, *ChJAA (Chin. J. Astron. Astrophys.)*, 5, 539
- Macario-Rojas, A., Smith, K. L., & Roberts, P. C. E. 2018, *MNRAS*, 479, 3791
- McKinnon, J. A., & Waldmeier, M. 1987, *Sunspot Numbers, 1610-1985: Based on the Sunspot Activity in the Years 1610–1960 (World Data Center A for Solar-Terrestrial Physics)*
- Miao, J., Wang, X., Ren, T.-L., & Li, Z.-T. 2020, *RAA (Research in Astronomy and Astrophysics)*, 20, 004
- Nandy, D., & Martens, P. C. H. 2007, *Advances in Space Research*, 40, 891
- Ohl, A. 1966, *Soln. Danye*, 12, 84
- Pesnell, W. D., & Schatten, K. H. 2018, *Sol. Phys.*, 293, 112
- Petrovay, K. 2010, *Living Reviews in Solar Physics*, 7, 6
- Petrovay, K. 2020, *Living Reviews in Solar Physics*, 17, 2
- Petrovay, K., Nagy, M., Gerják, T., & Juhász, L. 2018, *Journal of Atmospheric and Solar-Terrestrial Physics*, 176, 15
- Pishkalo, M. I. 2019, *Sol. Phys.*, 294, 137
- Podladchikova, T., Van der Linden, R., & Veronig, A. M. 2017, *ApJ*, 850, 81
- Sarp, V., Kilcik, A., Yurchyshyn, V., et al. 2018, *MNRAS*, 481, 2981
- Sello, S. 2019, *arXiv e-prints*, arXiv:1902.05294
- Sheeley, N. R., J. 2008, *ApJ*, 680, 1553
- Singh, A. K., & Bhargawa, A. 2017, *Ap&SS*, 362, 199
- Singh, A. K., & Bhargawa, A. 2019, *Ap&SS*, 364, 12
- Upton, L. A., & Hathaway, D. H. 2018, *Geophys. Res. Lett.*, 45, 8091
- Usoskin, I. G., & Mursula, K. 2003, *Sol. Phys.*, 218, 319
- Waldmeier, M. 1935, *Astronomische Mitteilungen der Eidgenössischen Sternwarte Zurich*, 14, 105
- Waldmeier, M. 1961, *The Sunspot-activity in the Years 1610–1960 (Zurich: Schulthess)*
- Wang, Y. M., & Sheeley, N. R. 2009, *ApJL*, 694, L11
- Wilson, R. M. 1995, *Sol. Phys.*, 158, 197
- Wilson, R. M., Hathaway, D. H., & Reichmann, E. J. 1996, *J. Geophys. Res.*, 101, 19967
- Yousef, S. 2003, in *ESA Special Publication*, 535, *Solar Variability as an Input to the Earth's Environment*, ed. A. Wilson, 177